

Development of CMOS Pixel Sensors fully adapted to the ILD Vertex Detector Requirements

Marc Winter, Jérôme Baudot, Auguste Besson, Gilles Claus, Andreï Dorokhov, Mathieu Goffe, Christine Hu-Guo, Frédéric Morel, Isabelle Valin, Georgios Voutsinas and Liang Zhang

Institut Pluridisciplinaire Hubert Curien (IPHC) - Université de Strasbourg
23 rue du loess, BP-28, 67037 Strasbourg Cedex 2 - France

CMOS Pixel Sensors are making steady progress towards the specifications of the ILD vertex detector. Recent developments are summarised, which show that these devices are close to comply with all major requirements, in particular the read-out speed needed to cope with the beam related background. This achievement is grounded on the double-sided ladder concept, which allows combining signals generated by a single particle in two different sensors, one devoted to spatial resolution and the other to time stamp, both assembled on the same mechanical support. The status of the development is overviewed as well as the plans to finalise it using an advanced CMOS process.

1 Introduction

The ILC physics programme encompasses numerous studies relying on high precision flavour tagging, including high quality charmed meson and tau lepton identification. This objective translates into the necessity of a very precise vertex detector, to be equipped with very granular and thin pixel sensors. Taking advantage of the ILC running conditions, which are much less demanding than those at the LHC, physics driven specifications such as spatial resolution can be privileged at the expense of read-out speed or radiation tolerance.

CMOS Pixel Sensors (CPS) constitute a category of Monolithic Active Pixel Sensors (MAPS) offering attractive features for such requirements. They easily match the targeted granularity and material budget, and do not necessitate a cooling system adding substantial material budget inside the fiducial volume of the detector. On the other hand, the hit rate generated by the beam related background in the innermost layer of the detector sets target values of the read-out speed which are not straightforward to achieve, given the size, and thus the number, of the pixels needed to match the spatial resolution. Speed is therefore a major driving parameter of the development of CPS since a few years.

2 State-of-the-art CPS

2.1 Sensor short description

The sensors MIMOSA-26 [1] and -28 [2] sensors may be considered as the state-of-the-art of the CPS technology for charged particle tracking. They were realised to equip the EUDET beam telescope [3] and the new STAR vertex detector [4], respectively. Their pixels are grouped in columns read out in parallel and terminated with an offset compensated discriminator. Inside each column, the pixels are read out sequentially with a typical read-out time of $\lesssim 200$ ns per pixel. This so-called *rolling shutter* mode exhibits the great advantage of limiting the power consumption of the whole pixel array to the amount needed to operate a single row. MIMOSA-26 and -28 exhibit power consumptions of about 250

and 150 mW/cm² respectively, the spread between both values reflecting the geometry differences of the two sensors.

The pixel pitch is around 20 μm for both sensors. Each pixel incorporates a micro-circuit allowing for correlated double-sampling for the purpose of average pixel noise subtraction, and a pre-amplification stage mitigating the impact of the noise sources of the signal processing chain downstream of the pixels. The discriminator thresholds, as well as the settings of most of the sensors' steering parameters, are remotely programmable through a JTAG circuitry integrated on the sensor. A zero-suppression circuit integrated in the chip periphery transforms the signals in excess of the discriminator thresholds into hit pixel addresses which are buffered in integrated SRAMs before being transmitted to the outside world.

3 Achieved detection performances

The detection performances of several tens of sensors were assessed with minimum ionising particle beams at CERN and DESY. Numerous measurements were performed with 50 μm thin sensors, at various operation temperatures and after exposures to various integrated ionising and non-ionising radiation doses. Figure 1 shows typical values of the detection efficiency, pixel fake hit rate (due to noise fluctuations above threshold) and single point resolution obtained with a MIMOSA-26 sensor at a temperature of about 20°C for various values of the discriminator thresholds.

One observes that the detection efficiency stays close to 100 % for threshold values high enough to keep the fake hit rate at a negligible level (e.g. $\lesssim 10^{-4}$). The single point resolution is only slightly in excess of the ILD specification of 3 μm [5]. It results from an impact position reconstruction based on the centre of gravity of the positions the few pixels composing a cluster. The value obtained is well below the digital resolution reflecting the 18.4 μm pixel pitch of MIMOSA-26 (i.e. 5.3 μm) despite the binary charge encoding. It follows that a pitch of $\lesssim 17 \mu\text{m}$ would allow complying with the 3 μm spatial resolution required for the ILD vertex detector. It was actually checked that the discriminators ending the columns would fit within $<17 \mu\text{m}$ wide columns. These performances hold for irradiated sensors (e.g. MIMOSA-28 was validated for 150 kRad and $3 \times 10^{12} \text{n}_{eq}/\text{cm}^2$ at a temperature of 30-35°C).

The 576 pixels composing the 1152, 10.5 mm long, columns of MIMOSA-26 are read out from one side in about 100 μs . The read-out would be twice faster, i.e. $\sim 50 \mu\text{s}$ short, in case of a double-sided read-out architecture where each column is split in two opposite halves. As explained later in this paper, this value is expected to be appropriate for the innermost layer of the ILD vertex detector, which is exposed to the highest particle rate. The twice

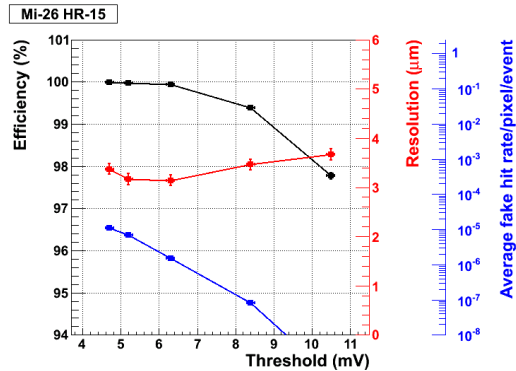


Figure 1: MIMOSA-26 beam test results obtained at the CERN-SPS with $\sim 10^2$ GeV charged particles. The detection efficiency (in black), the fake hit rate (in blue) and the single point resolution (in red) are shown for various values of the discriminator thresholds.

higher power consumption resulting from the double-sided read-out is still expected to be compatible with low mass air cooling.

4 Concept developed for the ILD vertex detector

As indicated in the previous section, the compliance of CPS with the single point resolution and the material budget specifications of the ILD vertex detector are not questionable. The measured radiation tolerance of MIMOSA-26 and -28 is also expected to be sufficient for the running conditions foreseen. The remaining questions are whether the read-out speed can accommodate the hit rate generated by the beam related background, and whether the power consumption is compatible with a non-disturbing cooling mean such as air flow.

The particle rate is dominated by beamstrahlung electrons, and decreases rapidly when moving away from the interaction region [5]. For instance, a detector geometry based on three cylindrical double-sided layers featuring average radii of 17, 38 and 59 mm, faces a hit density varying by one ordre of magnitude from one layer to the next. On the other hand, the innermost layer, which is by far the most exposed to beamstrahlung background, is also the smallest one, standing for only about 10 % of the total detector surface. These features are exploited in the concept developed here, together with the design flexibility and the moderate cost of the CPS technology.

Three different sensors are foreseen, each optimised for a different balance between the single point resolution, the read-out speed and the power consumption. The $\lesssim 3 \mu\text{m}$ resolution and the fast read-out needed for the innermost layer are provided by two different sensors, implemented on the two faces of the ladders equipping the layer.

One sensor, called MIMOSA-in, provides the spatial resolution with $17 \times 17 \mu\text{m}^2$ pixels read out in $\sim 50 \mu\text{s}$. The other sensor, called AROM^a, features $17 \times 85 \mu\text{m}^2$ pixels elongated in the direction of the columns. It is therefore read out in $\sim 10 \mu\text{s}$, the columns being composed of ~ 5 times less pixels. Based on beam test results of a sensor prototype featuring $18.4 \times 73.2 \mu\text{m}^2$ pixels, its spatial resolution is expected to be $\lesssim 6 \mu\text{m}$ in both directions with staggered pixels [6].

Particles traversing the layer will thus get assigned a spatial resolution of $\lesssim 3 \mu\text{m}$ combined with a $\sim 10 \mu\text{s}$ time stamp from their two, $\sim 2 \text{ mm}$ apart, impacts. The approach is illustrated in Figure2. The ambitionned ladder total material budget amounts to $\lesssim 0.3 \%$ of radiation length. Details on the ladder design and development may be found in [7].

The outer layers, which are less demanding in terms of spatial resolution and read-out speed, are foreseen to be equipped with a sensor consuming at least 3 times less power, called MIMOSA-out. It is supposed to provide a single point resolution of $\sim 4 \mu\text{m}$ and

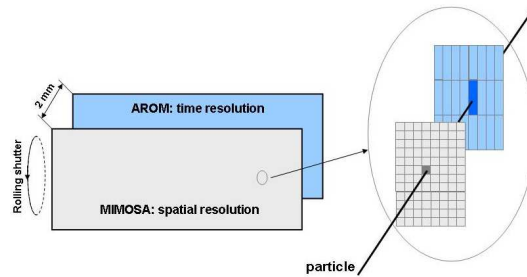


Figure 2: Schematic view of the combination of AROM (elongated pixels) and MIMOSA (square pixels) sensors equipping a 2 mm thick double-sided ladder.

^a AROM stands for Accelerated Read-Out MIMOSA sensor.

a read-out time of $\sim 100 \mu s$. The pixels are $34 \times 34 \mu m^2$ large, i.e. 4 times larger than the pixels of MIMOSA-in. Despite the sizeable pitch, a good spatial resolution is expected from replacing the discriminators ending the columns with $\lesssim 4$ -bit ADCs incorporating a discriminator stage. The zero-suppression circuitry of MIMOSA-in can easily be adapted to this change of the charge encoding.

The expected spatial and temporal resolutions of the three sensors are summarised on Table 1, where they are compared to the detector specifications. The latter are clearly within reach of the CPS proposed, which are not expected to face any challenge given the performances already achieved with existing sensors. The finalisation of the development is well under way and should converge within a few years, as explained in the next section.

5 Sensor finalisation plans

The development of the three sensors does not require the same effort for all of them. While MIMOSA-in and AROM are relatively straightforward to realise, MIMOSA-out still requires establishing the operation of fast ADCs ending the columns (and the corresponding zero-suppression micro-circuitry).

5.1 Validation of the sensor architectures

The validation of the architectures of MIMOSA-in and AROM motivated the realisation of the MIMOSA-30 prototype, which combines the two designs. It is split in two halves, each made of 128 columns ended with a discriminator. One half features columns of 256, $16 \times 16 \mu m^2$ large, pixels standing for a section of MIMOSA-in. The other half differs by the pixel size and number, i.e. the columns contain 64 elongated pixels of $16 \times 80 \mu m^2$, and stands for a section of AROM. The read-out times of the two halves amount to the nominal values of MIMOSA-in and AROM, i.e. about 50 and 10 μs respectively and the pixel dimensions were chosen to safely comply with the ILD spatial resolution requirement. The chip was fabricated at the end of 2011 and its performances are foreseen to be assessed at the CERN-SPS in Spring or Summer 2012.

The MIMOSA-out architecture, with its integrated ADCs, is being prototyped with the MIMOSA-31 chip, also fabricated by the end of 2011. The ADC design resembles the Successive Approximation Register architecture. It features a variable charge encoding granularity, ranging from a maximum of 4 bits for signals of small magnitude to only 2 bits for large signals. Earlier prototypes allowed to check that a rough encoding of the amplitude delivered by those pixels in a cluster having collected the largest charges does not degrade the resolution on the reconstructed impact position. The precise performances of the sensor will be investigated at the CERN-SPS in Autumn 2012.

Layer	Specs	MIMOSA	AROM
Inner	$\lesssim 3 \mu m$	$\lesssim 3 \mu m$	$\lesssim 6 \mu m$
	25-50 μs	50 μs	10 μs
Outer	$\lesssim 5 \mu m$	$\lesssim 4 \mu m$	–
	100-200 μs	100 μs	–

Table 1: ILD vertex detector specifications for the single point and time resolutions in the innermost and outer layers. The expected performances of the 3 sensors (MIMOSA-in and -out, AROM) proposed to equip the detector are shown in comparison.

5.2 Translation in an advanced fabrication process

Most of the sensors realised up to now, including MIMOSA-26 and -28 as well as MIMOSA-30 and -31 (see previous sub-section), were manufactured in a $0.35\ \mu\text{m}$ CMOS process. The latter is far from relying on fabrication parameters allowing to approach the real potential of the CPS technology. For instance, the number of metalisation layers, limited to 4, complicates substantially the integration of the ADCs in MIMOSA-out. The next steps of the development will therefore rely on a $0.18\ \mu\text{m}$ process, which features several improvements with respect to the $0.35\ \mu\text{m}$ process. Besides the improved ionising radiation tolerance consecutive to the thinner gate oxide, the process offers 6-7 metalisation layers and deep p-wells allowing to use both types of transistors inside the pixels without substantial parasitic charge collection by the n-type zones hosting P-MOS transistors.

The first prototype exploring this new technology was fabricated during the last quarter of 2011. It includes various pixel designs exploring different charge sensing and in-pixel amplification options. It will be followed in 2012 by prototypes reproducing the architectures of MIMOSA-30 and of the as the zero-suppression circuitry necessary to complete the final sensor design. Various architectures will actually be explored. Some of them are intended to squeeze the AROM read-out time to a few μs . One motivation for this short integration time is the necessity to accommodate the higher beamstrahlung background expected when the ILC will be running around 1 TeV collision energy. The short integration time is also relevant for the running at 500 GeV, for instance to mitigate the need for a dedicated solenoid installed inside the beam pipe to protect the vertex detector from low energy beam background electrons backscattered from beam elements located near the interaction point. If required, it would also allow for a higher granularity of the MIMOSA-in sensor, which would slow down its read-out speed.

Detailed estimates of the total power of the detector were performed with various sensor configurations and assumptions on the AROM sensor read-out speed. These computations indicate an instantaneous consumption in the order of 0.5 kW. Assuming a conservative sensor duty cycle of 2 %, while the machine duty cycle is about 0.5 %, the average power consumption of the whole detector would amount to $\sim 10\ \text{W}$. This value is expected to be modest enough to be compatible with an air flow based cooling system.

6 Summary

Three different CMOS pixel sensors are being developed for the ILD vertex detector, adapted to an original concept privileging the spatial and temporal resolutions in the innermost layer, and minimising the power consumption in the outer layers. Their development is well advanced, translating into the perspective of fabricating full scale prototypes complying with all detector specifications within the few coming years. In particular, the fast read-out imposed on the sensors equipping the innermost layer of the detector is nearly achieved, with the perspective of further improvements reducing the integration time to a few microseconds only, well beyond the requirements at a 500 GeV collision energy, but well suited to the machine operation near 1 TeV.

The finalisation of the development relies in particular on a $0.18\ \mu\text{m}$ CMOS process currently under study. This R&D programme is pursued in synergy with the ALICE-ITS upgrade effort [8] as well as in the perspective of the upcoming CBM experiment at FAIR [9], for which the fast variants of the AROM sensor are particularly attractive.

References

- [1] A. Dorokhov *et al.*, Nucl. Inst. & Meth. **A650**, 174 (2011).
- [2] I. Valin *et al.*, TWEPP-2011 Conf. Proc. (2011), to be pub. in JINST.
- [3] A. Besson *et al.*, arXiv:1201.4657v1 [physics.ins-det] (2011).
- [4] L. Greiner *et al.*, Nucl. Inst. & Meth. **A650**, 68 (2011).
- [5] ILD Concept Group, ILD Letter of Intent, arXiv:1006.3396v1 [hep-ex] (2010)
- [6] A. Besson *et al.*, ICHEP-2011 Conf. Proc. (2012).
- [7] J. Baudot *et al.*, these proceedings.
- [8] ALICE collaboration, ALICE-ITS upgrade Conceptual Design Report, (2012).
- [9] Ch. Schrader *et al.*, XLVIII Int. Winter Meet. on Nucl. Phys., Conf. Proc. (2010).